International Journal of Thermophysics, Vol. 10, No. 5, 1989

Nonequilibrium Molecular Dynamics Calculation of the Shear Viscosity of Carbon Dioxide[1]

B. Y. Wang[2] and P. T. Cummings[2]

Nonequilibrium molecular dynamics calculations of the shear viscosity of supercritical carbon dioxide along the 313 K isotherm are reported. Three different intermolecular potential models of increasing complexity are considered: a spherically symmetric Lennard–Jones potential, a two-site Lennard–Jones potential, and a three-site potential which includes a quadrupole–quadrupole moment. Results for the three potentials are compared with experimental data.

KEY WORDS: carbon dioxide; intermolecular potentials; molecular dynamics; supercritical fluids.

1. INTRODUCTION

In this paper, we begin a study of the transport properties of supercritical fluids and mixtures using the tool of nonequilibrium molecular dynamics (NEMD) [1]. The initial focus of the study is on the transport properties of supercritical, pure carbon dioxide, and this paper is devoted to an examination of the shear viscosity of carbon dioxide along the 313 K supercritical isotherm.

NEMD has recently emerged as one of the most efficient tools for calculating the transport properties of molecular fluids. (For a review of NEMD, see Evans and Morriss [1]. The most widely used alternative technique involves performing an equilibrium molecular dynamics and using the Green–Kubo equations for the transport properties. This approach is exemplified by the paper by Hoheisel in this volume.) In general, NEMD involves simulating a system at steady state away from

[1] Paper presented at the Tenth Symposium on Thermophysical Properties, June 20–23, 1988, Gaithersburg, Maryland, U.S.A.

[2] Department of Chemical Engineering, University of Virginia, Charlottesville, Virginia 22901, U.S.A.

0195-928X/89/0900-0929$06.00/0

equilibrium, where the steady state is attained through the application of an external field. The ratio of the field-induced current to the field itself gives the transport coefficient of interest. The sllod algorithm [2], described in Section 2, is used in conjunction with shearing boundary conditions to apply an external strain field to a fluid and thus permit the calculation of the shear viscosity from the ratio of the pressure tensor to the strain rate. The Newtonian viscosity is obtained as the zero-strain rate extrapolation of the strain rate-dependent shear viscosity.

Three intermolecular pair potential models for carbon dioxide are considered. The simplest model for CO_2 regards the molecule as spherically symmetric. The interaction potential is then a Lennard–Jones potential with parameters determined by fitting to the gas phase viscosity [3]. The second potential studied represents the next level of complexity: a two-site model in which the oxygen centers are explicitly modeled [4]. This model contains some of the elements of the shape of CO_2 but does not include the electrostatic interaction due to the permanent quadrupole moment of CO_2. The third potential is a three-site model (in which the centers of the oxygen and carbon atoms are explicitly represented) and the quadrupole–quadrupole interaction included [5]. The three potentials are described in detail in Section 2. The computational requirements for the NEMD simulation increase dramatically with the complexity of the potential model. The two-site model takes four times the computational time that the one-site (spherically symmetric) model requires; similarly, the three-site with quadrupole model takes 10 times longer than the one-site calculation. An appropriate question to ask is what complexity in pair potential is necessary to model supercritical transport properties effectively, and this is the motivation for considering three potential models of increasing complexity. For example, Simmons and Cummings [6] found that a five-site model for methane gave excellent results for the shear viscosity of supercritical methane at the state point they considered but that a one-site Lennard–Jones model yielded results within 12% of experiment at 1/25 of the computation cost. (Cummings [7] subsequently showed that the one-site model for methane was inferior to the full five-site model along the saturated liquid line.)

In Section 3, the shear viscosity of CO_2 obtained by NEMD at three densities along the 313 K isotherm is compared with experiment. Section 3 also contains conclusions drawn from the present study.

2. NEMD SIMULATION OF CARBON DIOXIDE

In this section, we briefly report the equations of motion used and the details of the pair potentials employed.

The sllod algorithm [2, 1] for simple fluids is described elsewhere; for molecular fluids, Simmons and Cummings [6] describe the major features of the algorithm. The equations of motion for a simulated system of N molecules with streaming velocity $\vec{u} = (\gamma y, 0, 0)$, where γ is the strain rate, are

$$\begin{aligned} d\vec{r}_i/dt &= \frac{\vec{p}_i}{m} + \vec{r}_i \cdot \nabla \vec{u} \\ d\vec{p}_i/dt &= \vec{F}_i - \vec{p}_i \cdot \nabla \vec{u} - \lambda \vec{p}_i \end{aligned} \tag{1}$$

$$\begin{aligned} d\vec{L}_i/dt &= \vec{T}_i \\ \vec{L}_i^p &= \mathbf{A}_i \vec{L}_i \\ \omega_{i\beta}^p &= L_{i\beta}^p / I_\beta, \qquad \beta = x, y, z \\ \frac{d}{dt}\begin{pmatrix} q_{i1} \\ q_{i2} \\ q_{i3} \\ q_{i4} \end{pmatrix} &= \frac{1}{2}\begin{pmatrix} -q_{i3} & -q_{i4} & q_{i2} & q_{i1} \\ q_{i4} & -q_{i3} & -q_{i1} & q_{i2} \\ q_{i1} & q_{i2} & q_{i4} & q_{i3} \\ -q_{i2} & q_{i1} & -q_{i3} & q_{i4} \end{pmatrix}\begin{pmatrix} \omega_{ix}^p \\ \omega_{iy}^p \\ \omega_{iz}^p \\ 0 \end{pmatrix} \end{aligned} \tag{2}$$

In these equations, for molecule i, $\vec{r}_i$, $\vec{p}_i$, $\vec{\omega}_i$, $\vec{L}_i$, $\vec{F}_i$, and $\vec{T}_i$ represent the position of the center of mass, translational momentum, angular velocity, angular momentum, force on the center of mass, and torque in the laboratory frame. The principal (or molecular) frame quantities have superscript p. The matrix $\mathbf{A}_i$ is the rotation matrix that converts the laboratory frame coordinates of molecule i to molecular frame coordinates and is a function of the orientation of the molecule. The q_{ij}, $j = 1,..., 4$ are the quaternions for representing the orientation of molecule i in such a way that the equations of motion are singularity-free [8]. The parameter λ is used to constrain the translational motion so that the translational kinetic energy is fixed at the required temperature. The functional form of the term involving λ follows from the application of Gauss's principle of least constraint [9] where the isokinetic constraint is

$$\frac{1}{2m}\sum_{i=1}^{N} \vec{p}_i^2 - \frac{3}{2} N k_B T = 0 \tag{3}$$

where k_B is Boltzmann's constant and T is the absolute temperature. This leads to the following equation for λ:

$$\lambda = \sum_{i=1}^{N} (\vec{p}_i \cdot \vec{F}_i - \vec{p}_i \vec{p}_i \bullet \nabla \vec{u}) \Big/ \sum_{i=1}^{N} \vec{p}_i^2 \tag{4}$$

where • indicates the full contraction of two second-order tensors and N is the number of molecules in the simulation cell. For the algorithm to be homogeneous, the boundary conditions must be consistent with the equations of motion. Thus, we employ the Lees–Edwards [10] "sliding brick" boundary conditions The fourth-order Gear's predictor corrector method described in detail by Evans and Morriss [1] is used to solve the equations of motion.

The pressure tensor $\mathbf{P}$ is calculated from the expression

$$\mathbf{P}V = m \sum_{i=1}^{N} (\vec{v}_i - \vec{u})(\vec{v}_i - \vec{u}) + \sum_{i=1}^{N} \vec{r}_i \vec{F}_i \tag{5}$$

where V is the volume of the system and $\vec{v}_i = \vec{p}_i/m$ is the intrinsic velocity of molecule i. The strain rate-dependent shear viscosity η is obtained from the constitutive relation [11],

$$\mathbf{P}_{xy}^{os} = -2\eta(\nabla \vec{u})_{xy}^{os} \tag{6}$$

where $\mathbf{A}^{os}$ denotes the symmetric, traceless part of the tensor $\mathbf{A}$. The strain rate-dependent shear viscosity, hydrostatic pressure $p = (1/3)\,\mathrm{Tr}(\mathbf{P})$, and configurational internal energy u^{conf} are fitted to the asymptotic expressions [12]

$$\eta = \eta_0 - \eta_1 \dot{\gamma}^{1/2} \tag{7}$$

$$p = p_0 + p_1 \dot{\gamma}^{3/2} \tag{8}$$

$$u^{conf} = u_0 + u_1 \dot{\gamma}^{3/2} \tag{9}$$

The quantities with zero subscript are the zero-strain rate quantities, so that η_0 is the Newtonian viscosity.

The general form of the intermolecular potential is given by

$$u(12) = \sum_{\alpha=1}^{m} \sum_{\beta=1}^{m} u_{\alpha\beta}^{LJ}(r_{\alpha\beta}) + u_{QQ}(12) \tag{10}$$

Table I. Intermolecular Potentials for Carbon Dioxide

Model	n	(ε/k) (K)	σ (Å)	Θ (DÅ)	l (Å)
Spherical [3]	12	190.0	3.996	0.0	0.0
Two-site [4]	9	182.0	3.331	0.0	2.32
Three-site [5]	12	29.0(C–C) 83.1(O–O)	3.126(C–C) 3.383(O–O)	−3.85	2.32

Table II. NEMD Results for the Lennard–Jones Simple-Fluid Model of CO_2 Along the 313 K Isotherm

ρ (kg · m^{-3})	γ^*	Time steps	p (atm)	$u^{conf}/(Nk_BT)$	η (cp)
199.8	1.44	20,000	89.72	−0.694	0.0120
	1.0	20,000	91.16	−0.689	0.0148
	0.64	30,000	89.85	−0.671	0.0170
	0.36	30,000	88.95	−0.682	0.0180
	0.16	80,000	92.35	−0.661	0.0197
840.8	1.44	20,000	1347.5	−2.495	0.114
	1.0	20,000	1248.8	−2.530	0.116
	0.64	30,000	1215.2	−2.545	0.123
	0.36	30,000	1202.9	−2.552	0.115
	0.16	80,000	1176.6	−2.561	0.105
992.1	1.44	20,000	2947.2	−2.750	0.184
	1.0	20,000	2780.8	−2.802	0.196
	0.64	30,000	2695.7	−2.832	0.199
	0.36	30,000	2661.0	−2.846	0.220
	0.16	40,000	2654.3	−2.850	0.226

Table III. NEMD Results for the Two-Site Model of CO_2 Along the 313 K Isotherm

ρ (kg · m^{-3})	γ^*	Time steps	p (atm)	$u^{conf}/(Nk_BT)$	η (cp)
199.8	1.44	20,000	45.2	−5.721	0.007
	1.0	20,000	24.4	−3.839	0.006
	0.64	20,000	25.5	−2.368	0.012
	0.36	20,000	24.5	−2.303	0.013
	0.16	20,000	37.8	−1.639	0.019
840.8	1.44	10,000	−366.2	−4.660	0.071
	1.0	20,000	−260.8	−4.679	0.065
	0.64	20,000	−320.1	−4.711	0.069
	0.36	20,000	−309.7	−4.707	0.068
	0.16	20,000	−286.0	−4.807	0.071
992.1	1.44	20,000	−172.9	−5.383	0.103
	1.0	20,000	−295.5	−5.433	0.101
	0.64	20,000	−295.4	−5.426	0.104
	0.36	20,000	−313.4	−5.467	0.098
	0.16	20,000	−305.3	−5.443	0.103

where m is the number of sites in the molecule, $r_{\alpha\beta}$ is the distance between site α and site β in distinct molecules, $u_{QQ}(12)$ is the quadrupole–quadrupole interaction between molecule centers and the site–site interaction $u_{\alpha\beta}^{LJ}(r)$ is a Lennard–Jones potential of the form

$$u_{\alpha\beta}(r) = \frac{\varepsilon_{\alpha\beta}}{(n-6)}\left[6\left(\frac{\sigma_{\alpha\beta}}{r}\right)^n - n\left(\frac{\sigma_{\alpha\beta}}{r}\right)^6\right] \tag{11}$$

In this equation, $\varepsilon_{\alpha\beta}$ is the well depth of the potential, $\sigma_{\alpha\beta}$ is the zero of the energy, and n is the power law for the repulsive energy. The distance between the oxygen atoms in the two- and three-site models is denoted by l. The three-site model has a point quadrupole moment at the molecular center of mass which coincides with the center of the carbon atom. The cross-interaction parameters ε_{co} and σ_{co} are obtain by the usual Berthelot combining rules

$$\varepsilon_{CO} = (\varepsilon_{OO}\varepsilon_{CC})^{1/2}, \qquad \sigma_{CO} = \tfrac{1}{2}(\sigma_{OO} + \sigma_{CC}) \tag{12}$$

The parameters for the models are listed in Table I.

3. RESULTS

In Tables II, III, and IV, we report the pressure, configurational internal energy, and viscosity for the one-site, two-site, and three-site models of

Table IV. NEMD Results for the Three-Site Model of CO_2 Along the 313 K Isotherm

ρ (kg · m^{-3})	γ^*	Time steps	p (atm)	$u^{conf}/(Nk_BT)$	η (cp)
199.8	1.44	20,000	81.0	−1.030	0.0093
	1.0	20,000	73.8	−1.188	0.0105
	0.64	20,000	78.7	−0.939	0.0134
	0.36	20,000	79.7	−0.945	0.0188
	0.16	20,000	82.3	−0.922	0.0190
840.8	1.44	20,000	468.6	−3.240	0.0714
	1.0	20,000	402.9	−3.236	0.0752
	0.64	20,000	380.6	−3.298	0.0733
	0.36	20,000	349.5	−3.296	0.0739
	0.16	20,000	399.3	−3.303	0.0754
992.1	1.44	20,000	954.6	−3.826	0.107
	1.0	20,000	817.4	−3.903	0.111
	0.64	20,000	736.3	−3.906	0.116
	0.36	20,000	745.6	−3.915	0.123
	0.16	20,000	726.8	−3.937	0.121

CO_2, respectively. The simulations of the one-site model were performed on systems of 108 molecules with time step 1.32×10^{-14} s; the simulations of the two- and three-site models were performed on systems of 125 molecules with time step $\Delta t = 10^{-15}$ s for five reduced strain rates $\gamma^* = \gamma\sigma(m/\varepsilon)^{1/2} = 0.16$, 0.36, 0.64, 1.0, and 1.44. The spherical cutoff of the intermolecular potential is 12 Å for the one-site simulations and 10 Å for the two-site and three-site models. The longest computations (three-site model and some two-site) were performed on a CSPI 6420 64-bit word array processor (attached to a Prime 850 located in the Center for Computer-Aided Engineering at the University of Virginia) and on a Cyber 180/855 (located in the Academic Computing Center at the University of Virginia). The shorter simulations (one-site and some two-site) were performed on the Prime 850 noted above and on two Sun 3 workstations.

The strain rate-dependent pressure, shear viscosity, and configurational internal energy were least squares fitted to the asymptotic formulae given in Eqs. (7)–(9). Figures 1–3 show the strain rate-dependent viscosity

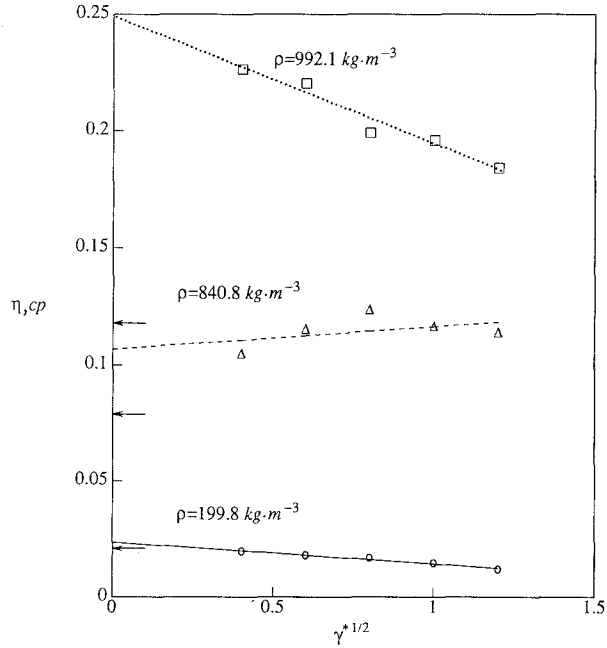

Fig. 1. The viscosity η for the one-site model of CO_2 at densities 199.8, 840.8, and 992.1 kg · m^{-3} along the 313 K isotherm as a function of $\gamma^{*1/2}$. The symbols are simulation results (to which the straight lines are least-squares fits) and the arrows indicate the experimental data.

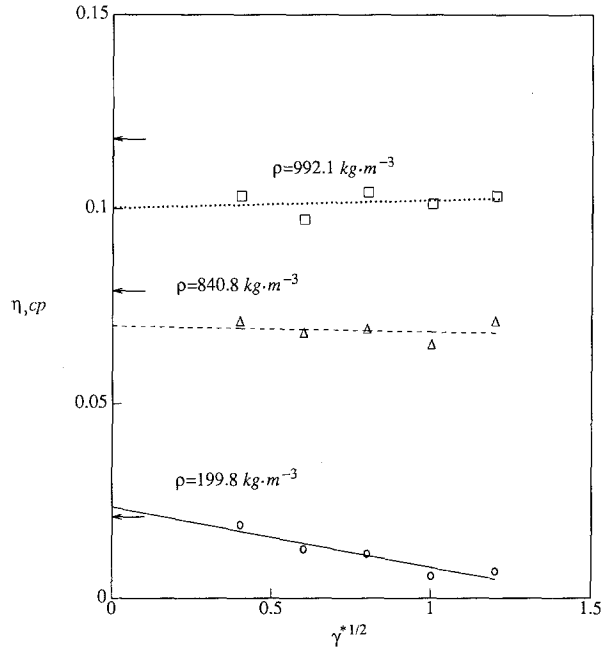

Fig. 2. The viscosity η for the two-site model of CO_2 at densities 199.8, 840.8, and 992.1 $kg \cdot m^{-3}$ along the 313 K isotherm as a function of $\gamma^{*1/2}$. The symbols, lines, and arrows have the same significance as in Fig. 1.

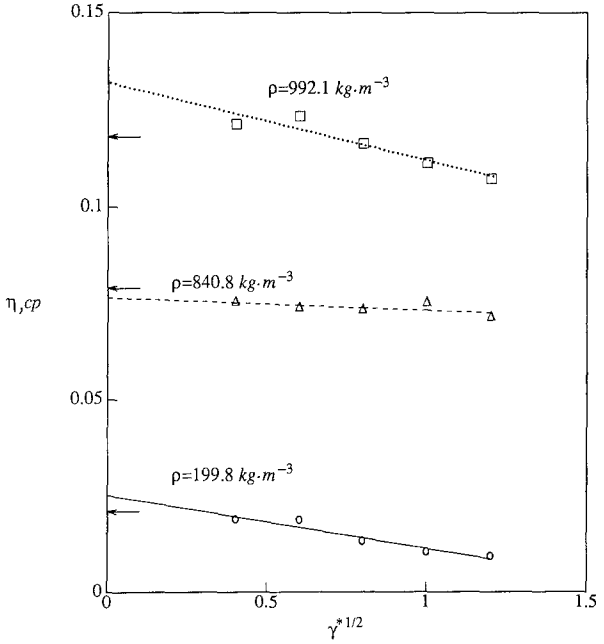

Fig. 3. The viscosity η for the three-site model of CO_2 at densities 199.8, 840.8, and 992.1 $kg \cdot m^{-3}$ along the 313 K isotherm as a function of $\gamma^{*1/2}$. The symbols, lines, and arrows have the same significance as in Fig. 1.

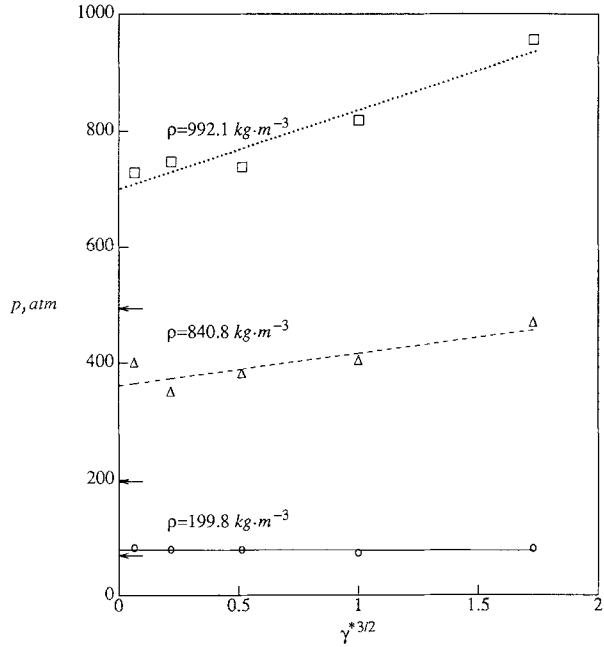

Fig. 4. The pressure p for the three-site model of CO_2 at densities 199.8, 840.8, and 992.1 kg · m^{-3} along the 313 K isotherm as a function of $\gamma^{*3/2}$. The symbols, lines, and arrows have the same significance as in Fig. 1.

for the each of the potential models along the 313 K isotherm. The viscosity follows the asymptotic relation (7) quite well. The strain rate-dependent pressure and configurational internal energy for the three-site model are shown in Figs. 4 and 5; again, the asymptotic formulae evidently fit the simulation results well.

4. CONCLUSIONS

The NEMD results for the three-site model are in very good agreement with the experimental results on the shear viscosity and in reasonable agreement with the experimental pressures. The simple fluid model results are in good agreement at the lowest density (as is expected since the parameters in the potential are fitted to the zero density viscosity) but overestimate the viscosity and pressure as the density increases. The two-site model yields reasonable results for the viscosity, but the pressures are

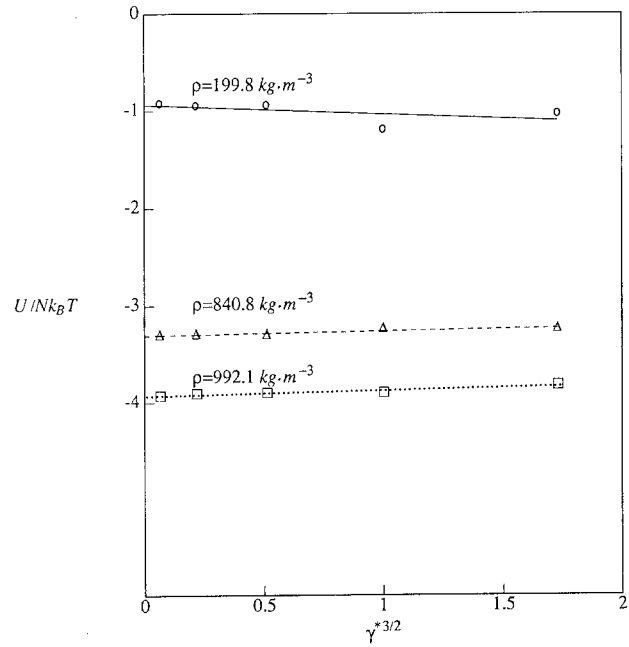

Fig. 5. The configurational internal energy u^{conf} for the three-site model of CO_2 at densities 199.8, 840.8, and 992.1 $kg \cdot m^{-3}$ along the 313 K isotherm as a function of $\gamma^{*3/2}$. The symbols and lines have the same significance as in Fig. 1.

Table V. Comparison Between Pressure and Shear Viscosity Calculated via NEMD and Experimental Data [13]

ρ ($kg \cdot m^{-3}$)	Model	p_{NEMD}	p_{exp}	η_{NEMD}	η_{exp}	$u^{conf}/(Nk_BT)$
199.8	One-site	90.8	69.1	0.024	0.0210	−0.668
	Two-site	—		0.024		−1.485
	Three-site	79.8		0.025		−0.937
840.8	One-site	1170	197.4	0.107	0.0792	−2.563
	Two-site	—		0.070		−4.760
	Three-site	361.5		0.077		−3.306
992.1	One-site	2622	493.5	0.249	0.118	−2.859
	Two-site	—		0.100		−5.459
	Three-site	699.8		0.132		−3.939

negative. [In fact, the negative pressures fail to follow the $\gamma^{3/2}$ asymptotic formula and so no zero-strain rate extrapolation of these pressures is provided in Table V.] This indicates that the two-site model may be in the two phase region at the temperatures and densities studied, which implies that the two-site model fluid in this case is not supercritical at 313 K.

In Section 1, a question about the complexity of the pair potential required in order to give accurate transport properties was raised. The results presented in this paper suggest that using the three-site model is capable of predicting accurate shear viscosities for supercritical carbon dioxide but that the other two, simpler models are not sufficiently accurate at high densities. It is clear that shape is playing an important role in determining the shear viscosity, since only the models with a nonspherical shape yield reasonable results for η over all three densities. The pressure, which in general is very sensitive to the attractive interactions, is best predicted when the electrostatic quadrupole–quadrupole is included.

The next steps in our study of supercritical fluids will include evaluating the three-site potential for diffusivity and thermal conductivity and using NEMD to calculate supercritical mixtures with carbon dioxide as the solvent.

ACKNOWLEDGMENTS

The authors gratefully acknowledge the support of this research by the National Science Foundation through Grant CBT-8613614 and through equipment Grant CPE-8405715, which provided matching funds for the purchase of the CSPI 6420 array processor used in this research.

REFERENCES

1. D. J. Evans and G. P. Morriss, *Comp. Phys. Rep.* **1**:297 (1984).
2. The earliest reference to the sllod algorithm is attributed to W. G. Hoover and A. J. C. Ladd (private communication) by D. J. Evans and G. P. Morriss, *Phys. Rev. A* **30**:1528 (1984).
3. R. B. Bird, W. E. Stewart, and E. N. Lightfoot, *Transport Phenomena* (Wiley and Sons, New York, 1960), Appendix B.
4. T. G. Gibbons and M. L. Klein, *J. Chem. Phys.* **60**:112 (1974).
5. C. S. Murthy and K. Singer, *Mol. Phys.* **44**:135 (1981).
6. A. D. Simmons and P. T. Cummings, *Chem. Phys. Lett.* **129**:92 (1986).
7. P. T. Cummings (in press).
8. D. J. Evans, *Mol. Phys.* **34**:317 (1977).
9. D. J. Evans, W. G. Hoover, B. H. Failor, B. Moran, and A. J. C. Ladd, *Phys. Rev. A* **28**:1016 (1983).

10. A. W. Lees and S. F. Edwards, *J. Phys. C* **5**:1921 (1972).
11. D. J. Evans, *J. Stat. Phys.* **20**:547 (1979).
12. K. Kawasaki and J. D. Gunton, *Phys. Rev. A* **8**:2048 (1973); T. Yamada and K. Kawasaki, *Prog. Theor. Phys.* **53**:1111 (1975); M. H. Ernst, B. Cichocki, J. R. Dorfman, J. Sharma, and H. van Beijeren, *J. Stat. Phys.* **18**:237 (1978); D. J. Evans, *J. Chem. Phys.* **78**:3297 (1983).
13. N. B. Vargaftik, *Handbook of Physical Properties of Liquids and Gases*, 2 ed. (Hemisphere, New York, 1983).